

Dear Members,

With new consortium research staff coming on board, we're expanding our research portfolio into some novel areas. We'll be delving into the challenges of flexible substrate assembly and thin die flip chip. On that front, work will begin using a relatively familiar metallized polyimide flex substrate material and progress into the more undefined and unfamiliar joining processes required for low temperature polymeric flex materials such as PET and PEN. Another new assembly process venture for us will be selective area laser reflow. If you've attended recent consortium meetings you'll recall that we've already had opportunity to examine laser reflowed flip chip connections in some detail. We'll soon be able to explore the process side as well. A selective area laser reflow tool is now being installed in our laboratory for our own experimentation and that of our consortium members.

The next AREA consortium meeting is scheduled for June 14th. Please plan to attend. It will be held in conjunction with the iMAPS *Advances in Semiconductor Packaging* workshop on June 15th. This annual iMAPS packaging workshop immediately follows our consortium meeting and will be held in the same Binghamton University venue. The workshop host, the Empire State chapter of iMAPs, has agreed to permit AREA consortium members access to the event. Be sure your travel plans allow you to stay for this second full day of technical content. The 2017 iMAPS workshop agenda is yet to be finalized but if previous years are any indication (e.g., [2016](#)), the event will share new insights on the latest in packaging design, materials, process and reliability—certainly worth that additional day.

Sincerely,
Jim Wilcox
Consortium Manager

APD11A,B. Laser Selective Reflow Soldering

A laser selective reflow soldering tool is now being installed in the APL. It will be fully operational in mid-May. In this unit, localized solder reflow is accomplished through the controlled impingement of a 980nm (IR) laser. Custom beam shaper optics redistribute the gaussian spot beam to a user selected uniform rectangular area beam. This selectable incident area ranges from 4×4mm to 100×200 mm. Beam power is controlled from 50 to 2000W.

This is a development tool. The covers are off, giving us engineering access to workpiece support tooling, positioning, and temperature measurement. We plan to explore the soldering process in some detail.

We already have several product specific trials proposed to us our by our consortium members. If you have ideas on novel processes, joining materials, or assembled structures that may be enabled by this tool please contact us.



Laser selective reflow tool being installed in the APL.

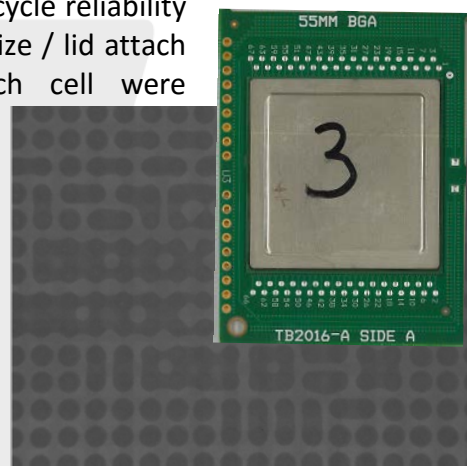
APD3B. Large Body BGA Assembly and Reliability



Lidless multi-chip and single chip FC-PBGAs assembled to a board.

Large body (55mm) FC-PBGA components had been fabricated earlier using thin core (600µm) laminate substrates. The substrate was a 0.8mm pitch full array laminate with 4356 I/O. Components were made in six different configurations, including 20mm and 35mm single die or 14×12mm multi-die (4-up) arrangements. Four configurations were fabricated with 40gm coined copper heatspreader lids. Two were lidless.

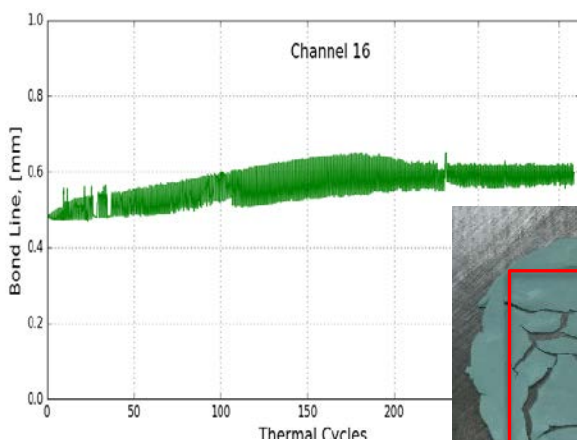
In preparation for a thermal cycle reliability comparison among the various die size / lid attach configurations, samples from each cell were assembled to test boards. All specimens with smaller die and no copper lid passed x-ray inspection and electrical test. The two cells having both a 35mm die and a copper lid however were prone to severe solder joint bridging under the die region, presumably due to some combination of the large die induced warpage during reflow and the total package weight.



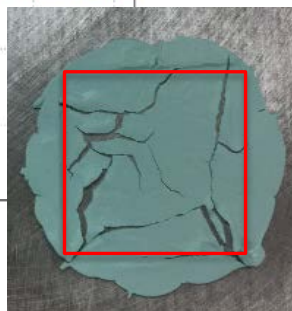
X-ray of BGA joints bridging under the 35mm die region of a lidded component (inset) as soldered to the test board.

MAT4C. TIM2 Thermal Cycle Reliability with Common Heatsink

Four thermal interface putty materials were evaluated for thermal cycle stability in a simulated large PCB assembly: Chomerics Gel 30, Laird 508, Jones 21-340E and Timtronics 5W. Sixteen component level nickel plated copper heat spreaders were adhesively attached along the diagonals of a blank 440×590×6.4 mm PCB. Each of the four TIMs was deposited on four of the component level heat spreaders along a half diagonal. A large aluminum plate heat spreader was mated to the array of component heat spreaders and fastened to the PCB with screws. Spacers at each screw location controlled the bondline at each site to the target 0.5mm. Electrical capacitance was measured across each of the TIM bondlines during thermal cycle.



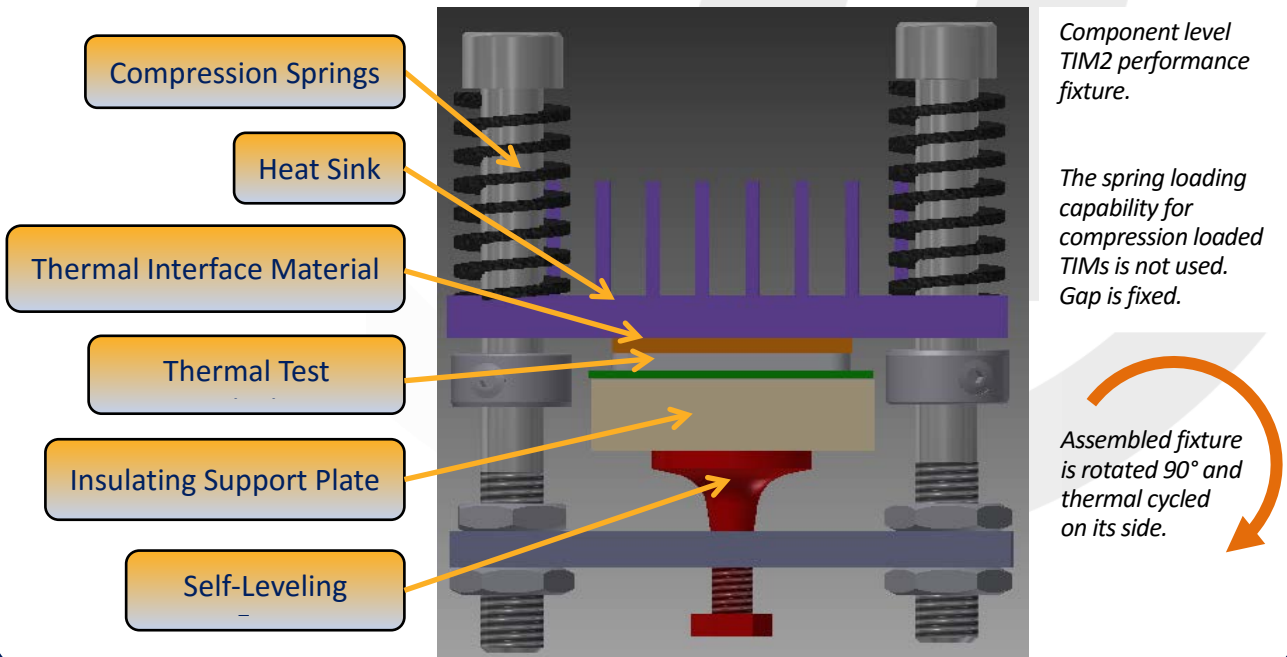
Cracks in TIM after 300 thermal cycles (40.5x40.5mm component indicated).



Changes in capacitance are indicative of geometric changes in the TIM bond. Plotted at left is the pseudo-bondline calculated from the capacitance response for the Jones 21-340E bond at the outermost, highest cyclic shear strain location. After 300 thermal cycles, the Jones 21-340E TIM shows cracks consistent with the measured reduction in capacitance. The effect of these cracks in reducing the capacitance is portrayed in the plot as an increasing bond line.

MAT4B. Component Level Testing of Thermal Interface Materials

Component level stability testing is being conducted on new generation thermal interface materials used between a lidded single chip module and a discrete aluminum heat sink. Two silicone putties and one non-silicone putty are being evaluated for stability of thermal performance using a -40 to 125 C accelerated thermal cycle. We are using our previously designed component TIM test fixture but without the spring loading feature. Instead the bond line is set at a fixed gap. The target bond line thickness is 0.4 to 0.5 mm. Thermal resistances on the order of 200°C mm²/W were measured for these TIMs in the assembled time zero condition. During thermal cycling, the TIM test structure is oriented on its side to emulate a vertical edge mount board application and observe whether gravity has a measurable effect on sag of the interface material. Dielectric constants were measured for all three materials enabling average bond lines to be calculated from the measured capacitance between the heat spreader and heat sink. Bond lines based on this capacitance calculation were around 0.4 mm.



MAT7H. Component Underfill for Low Melt Solder Drop Shock Enhancement

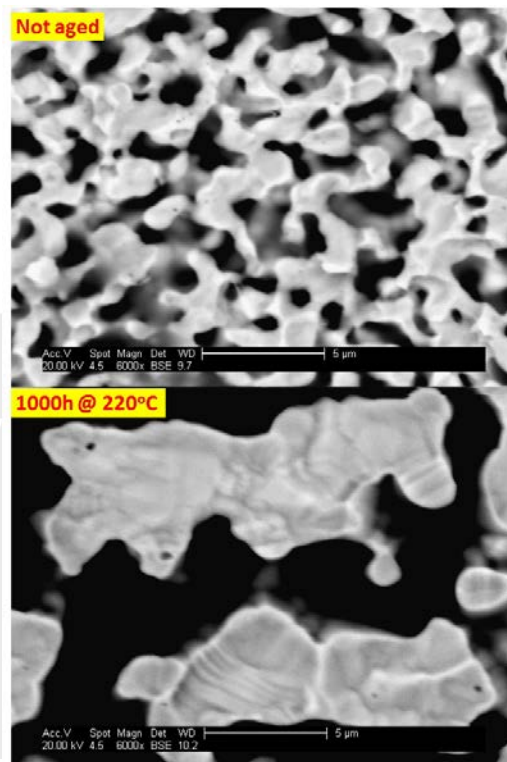
We previously reported very poor performance of BiSn eutectic solders in drop shock. With 900G drops, both BiSn and BiSnAg alloy joints failed within single digit drop counts. Electrically monitored CABGA 256 components attached with these alloys consistently failed with board side interfacial IMC cracks in the corner joints. A reduced shock loading of 500G, resulted in only marginally better performance of this interconnect; all parts still failing at less than 20 drops. Extended reflow profile provided no improvement for either alloy.

Component underfill was found to be quite effective in extending drop shock lifetime of these fragile BiSn interfaces. Testing the same experimental matrix of BiSn alloy and reflow profile produced a consistently robust drop shock result. All underfilled CABGA 256 samples survived 700 drops at 900G without fail before the test was ended. Similarly, 1500G drops were tolerated without fail through 250 drops when using component underfill.

MAT6B. Sintered Silver Die Attach

Samples consisting of Au-finish die attached to ImmAg or ENIG finish substrates using the micro-silver paste of the previously described experiments (Paste A) have been aged at 220°C for 500 and 1000 hours. This reduced aging temperature did not damage the substrate as much as 250°C aging had, allowing shear strength tests to be performed. Aging substantially reduced the strength of the bonding to both Ag and Au finishes but to a different extent for each material, causing a change in the preferred location of the shear separation between aged and non-aged samples. Microstructural analysis revealed a significant increase in the average pore size after aging (image at right).

An alternate nano-scale silver paste (Paste B) has since been acquired. In addition to the silver nanoparticles, this paste contains micron scale silver particles as filler. Its evaluation will generally follow the same approach as that used for Paste A. Preliminary tests performed include TGA (volatile mass loss rate with temperature), DSC (temperature range of volatile evaporation and sintering), and density measurements of sintered paste (porosity estimation).



Dramatic coarsening of pore sizes in sintered silver microstructures during thermal aging [before & after images at same magnification].

MAT8D. Conformal Coating for Mitigation of Sulfur Induced Resistor Corrosion

Board level assembly processes for the 2017 conformal coating evaluations are complete—for both the thermal cycle reliability impact test and the newly designed test coupon for flowers of sulfur corrosion testing—components are attached, jumpers soldered, and probe points masked. Boards are now being shipped to various providers for professional coating application.

Coating Materials

Humiseal 2A53

Humiseal 1B59LU

3M Novec 2708

EMCAST 1902

EMCAST 1916

Semblant MobileShield

AIT CC7130-PR

The seven coating materials selected for corrosion resistance testing are listed at left. A subset of that list (five) will be chosen for ATC reliability testing. Thermal cycling will be done using the TB2015 panel with CSP, BGA, QFN and LGA componentry. Direct comparison of results with earlier coating evaluations will thus be possible.

New resistor corrosion coupon; fully assembled with probe points masked prior to conformal coating.

(1 of 3 coupons shown)

